Journal of the Serbian Chemical Society
JSCS-info@shd.org.rs • www.shd.org.rs/JSCS
J. Serb. Chem. Soc. 81 (5) 553–566 (2016) UDC 546.26–162+66.087:544.4–44:621.397.3
JSCS–4867 *Original Scientific paper*

Relationship between the kinetic parameters and morphology of electrochemically deposited lead

NEBOJŠA D. NIKOLIĆ[1]*[#], PREDRAG M. ŽIVKOVIĆ[2], SANJA I. STEVANOVIĆ[1#] and GORAN BRANKOVIĆ[3]

[1]*ICTM-Department of Electrochemistry, University of Belgrade, Njegoševa 12, P.O.B. 473, 11001 Belgrade,* [2]*Faculty of Technology and Metallurgy, University of Belgrade, Karnegijeva 4, P.O.B. 3503, 11001 Belgrade and* [3]*Institute for Multidisciplinary Research, University of Belgrade, Kneza Višeslava 1a, Belgrade, Serbia*

(Received 18 December 2015, revised 12 February, accepted 19 February 2016)

Abstract: The processes of lead electrodeposition from electrolytes of various concentrations of sodium nitrate as the supporting electrolyte have been examined by chronoamperometry and by the scanning electron microscopic (SEM) analysis of deposits obtained in the potentiostatic regime of electrolysis. The good agreement between the diffusion coefficents determined by Cottrell equation and non-linear fitting method was observed. For the first time, the transition from the mixed ohmic-diffusion to the full diffusion control was defined from the analysis of Cottrell equation. The parameters, such as the number density of active sites and the nucleation rate constant, obtained by non-linear fitting method were discussed in accordance with the fact that lead belongs to the group of metals characterized by the high values of the exchange current density. The data obtained by the chronoamperometric analysis were succesfully correlated with morphologies of electrodeposited lead obtained in the different types of electrodeposition control.

Keywords: electrodeposition; chronoamperometry; diffusion; Cottrell equation; scanning electron microscope (SEM).

INTRODUCTION

Electrodeposition technique is very suitable way to synthesize metal of the desired characteristics and morphological forms.[1] In the dependence of regimes and parameters of electrolysis, such as applied current density or overpotential, composition and type of electrolytes, temperature of electrolysis, the type of working electrode, time of electrolysis, *etc*., metals can be obtained at both micro and nano scale in various forms including both compact and disperse (powder)

* Corresponding author. E-mail: nnikolic@ihtm.bg.ac.rs
[#] Serbian Chemical Society member.
doi: 10.2298/JSC151218028N

forms. Morphology of metal deposits also depends on the nature of metals, and metals are usually classified according to the general kinetic behaviour in aqueous solution on normal, intermediate and inert metals.[2,3] For example, the affiliation to the determined group of metals results in the different shapes of powder particles characterizing each of these groups.[4–7] Simultaneously, metals from the group of normal ones cannot be obtained in the compact form without use of additives, while electrodeposition of inert metals occurs in the whole range of potentials and current densities together with hydrogen evolution.

The metals from the group of normal metals are characterized by the high values of the exchange current density ($j_0 \rightarrow \infty$), low melting points and high overpotentials for hydrogen discharge.[2–4] The basic characteristics of the electrochemical processes of normal metals are fast charge-transfer step and the existence of the ohmic control in the initial part at the polarization curve.[8–10] Lead is the typical representative of normal metals which attracts both academic and technological attention thanking its specific characteristics, such as extremely high reactivity and superconductivity.[11] The electrolysis from the aqueous electrolytes is the most often used way to obtain Pb in the form suitable for some of above mentioned applications. The different electrolytes including both acid[9,10,12–15] and alkaline[16–18] ones are widely used for the processes of Pb electrodeposition. In the last time, electrolysis from choline chloride-urea deep eutectic solvents also uses to obtain Pb in the desired form.[19,20]

The various irregular forms of lead from granules and wires at sub-micrometer or nanometer scale to dendrites of the different shape are obtained by the processes of electrochemical deposition in the whole range of current densities or overpotentials.[9,10,11,21–26] Morphology of electrodeposited lead is strictly related with the type of electrodeposition control and the correlation between the polarization characteristics and formation of the determined morphological forms was established.[4,9,10,27] So the crystals of hexagonal shape are formed by the electrodeposition at overpotentials belonging to the ohmic control. On the other hand, elongated crystals known as precursors of dendrites, the needle-like and the branchy dendrites were formed during diffusion controlled electrodeposition.[9,10,27] Simultaneously, the shape of dendrites depends on the kind of electrolytes. The very branchy dendrites belonging to secondary (S) or tertiary (T) types in Wranglen`s definition of dendrites[28] were formed by electrodepositions from complex electrolytes, such as acetate (acid)[12] and hydroxide (alkaline)[18] electrolytes. Unlike of these very branchy dendrites, the needle-like and primary (P) dendrites were predominately electrodeposited from the basic nitrate electrolytes.[10,21]

Influence of regime and parameters of electrolysis on morphology of lead deposits has been examined in detail and systematized.[29] On the other hand, there is no many data related with kinetic parameters of Pb electrodeposition pro-

cesses.[30] In this study, the special attention will be devoted to the determination of kinetic parameters of the electrodeposition processes and the results obtained in this investigation will be correlated with the already existing knowledges. In this way, the completed insight in mechanism of Pb electrodeposition processes, as the typical representative of the very fast electrochemical processes, will be obtained. This will be done through the analysis of the effect of supporting electrolyte on the Pb electrodeposition processes from the nitrate electrolytes.

EXPERIMENTAL

Electrodeposition of lead was performed in an open cell at the room temperature from the following solutions: a) 0.10 M $Pb(NO_3)_2$ in 0.50 M $NaNO_3$, b) 0.10 M $Pb(NO_3)_2$ in 2.25 M $NaNO_3$ and c) 0.10 M $Pb(NO_3)_2$ in 4.0 M $NaNO_3$.

Doubly distilled water and analytical grade chemicals were used for the preparation of the solutions for the electrodeposition of lead. All electrodepositions were performed on vertical cylindrical copper electrodes. The geometric surface area of copper electrodes was 0.25 cm^2. The reference and counter electrodes were of pure lead. The counter electrode was a lead foil with a surface area of 0.80 dm^2 that was placed close to the cell walls. The reference electrode was a lead wire the tips of which were positioned at a distance of about 0.2 cm from the surface of the working electrodes. The working electrodes were placed in the center of a cell, at the same location for each experiment.

Polarization curve for electrodeposition of lead was recorded potentiostatically by changing overpotential in 5 mV steps. In order to obtain a reproductive shape of the polarization curves for this reaction, the following experimental procedure[5,10] usual for the recording of the polarization curves of fast electrodeposition processes, was applied. At low overpotentials the values of the current obtained after reaching steady-state values were used for constructing the polarization curves. Since at the overpotentials after the inflection point the current increased dramatically over time, the values recorded immediately after setting the selected overpotential values were used.

The potentiostatic current transients were recorded using Autolab potentiostat/galvanostat PGStat 128N (ECO Chemie, the Netherlands).

For the morphological analysis of lead deposits, lead was electrodeposited potentiostatically using a Wenking potentiostat/galvanostat – model 68 FR 0.5 at overpotentials of 20, 50 and 80 mV from 0.10 M $Pb(NO_3)_2$ in both 0.50 and 4.0 M $NaNO_3$ with the following quantities of electricity: 1.33 mA h cm^{-2} at 20 and 50 mV, and 0.55 mA h cm^{-2} at 80 mV. The obtained lead deposits were examined using a scanning electron microscope – Tescan digital microscope.

RESULTS AND DISCUSSION

Polarization characteristics

Polarization curves for Pb electrodeposition from solutions containing 0.10 M $Pb(NO_3)_2$ in various concentrations of $NaNO_3$ as the supporting electrolyte (0.50, 2.25 and 4.0 M $NaNO_3$) are shown in Fig. 1. The linear dependencies of the current density on the overpotential correspond to the ohmic control, and the length of linear parts at the polarization curves decrease with increasing $NaNO_3$ concentration. The ends of the ohmic control are denoted by vertical lines in Fig.

1. After the ohmic control, the electrodeposition systems enter the diffusion control, and the overpotentials up to the inflection points are characterized by dendritic growth inside the diffusion layer of the macroelectrode.[1,12, 31–33] After the inflection points, the electrodeposition systems remain the diffusion controlled and the rapid increase of the current density with increasing the overpotential is a consequence of the fast growth of dendrites which cause the strong increase of the electrode surface. In this zone, the outer limit of the diffusion layer of the macroelectrode is disrupted and this fast increase in the current density is ascribed to the activation controlled electrodeposition at the tips of growing dendrites.[1,12,31–33]

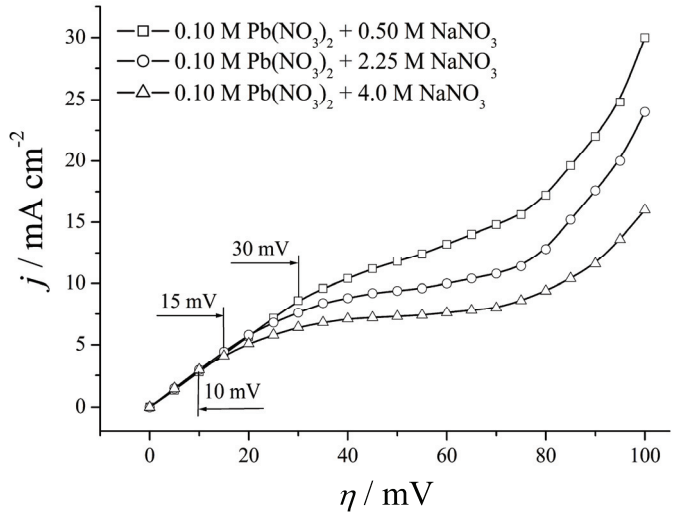

Fig. 1. Polarization curves for electrodeposition of lead from 0.10 M $Pb(NO_3)_2$ in 0.50, 2.25 and 4.0 M $NaNO_3$.

Determination of kinetic parameters of Pb electrodeposition processes

The analysis of chronoamperometry data based on Cottrell equation is widely used way for the determination of kinetic parameters of the electrodeposition processes. The potentiostatic current transients recorded from electrolytes containing 0.10 M Pb^{2+} in 0.50, 2.25 and 4.0 M $NaNO_3$ at overpotentials of 20, 35, 50, 65 and 80 mV are shown in Fig. 2. At the first sight, aside from the potentiostatic current transient obtained at 20 mV from the electrolyte with the addition of 0.50 M $NaNO_3$, the other potentiostatic current transients seems as the typical diffusion-limited ones.[30] The characteristics of these current transients are the increase in the current density up to the maximum, j_m, reached in a time, t_m, and the fall in the current density occuring after it. The rise in the current density up to maximum corresponds to either the independent growth of existing

nuclei or formation of new nuclei at the electrode surface, while the descending part in the potentiostatic current transients ascribes to linear diffusion to the planar electrode, described by the Cottrell equation.[30] The decrease in current density is sharper with the increase of both the overpotential and $NaNO_3$ concentration, *i.e.* with a strengthening of the effect of diffusion. From Fig. 2, it can be noticed that the j_m increases as t_m decreases with the shift to the higher applied overpotentials.

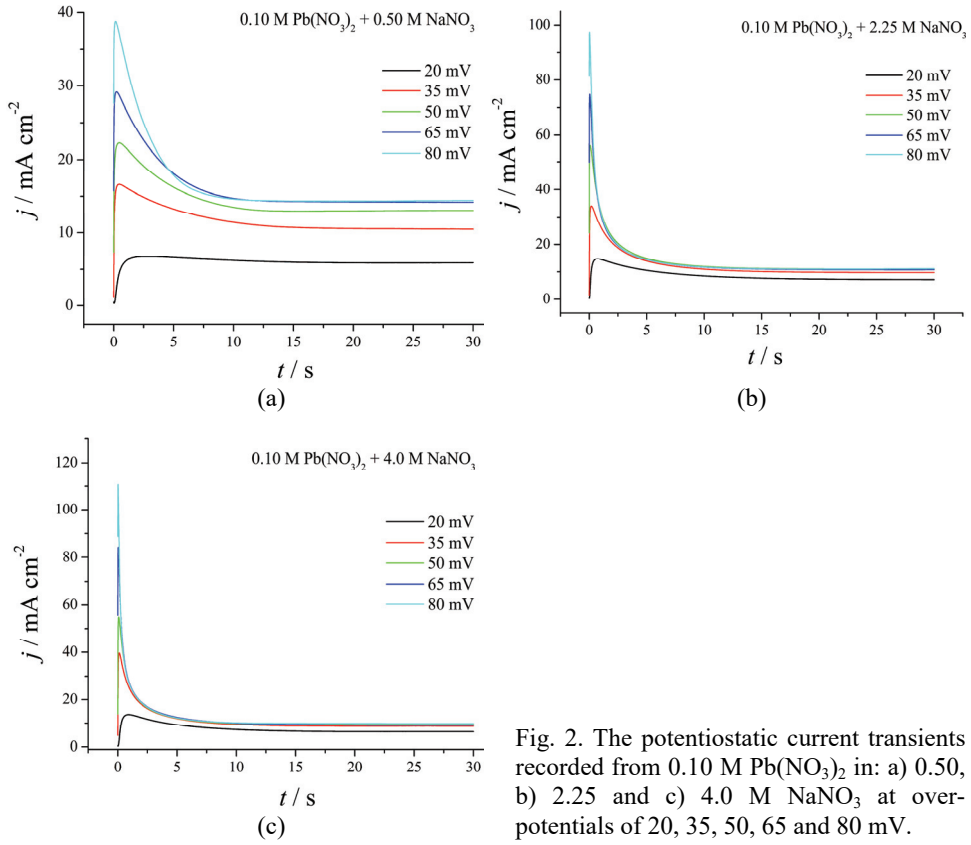

Fig. 2. The potentiostatic current transients recorded from 0.10 M $Pb(NO_3)_2$ in: a) 0.50, b) 2.25 and c) 4.0 M $NaNO_3$ at overpotentials of 20, 35, 50, 65 and 80 mV.

On the other hand, the potentiostatic current transient recorded from 0.10 M Pb^{2+} in 0.50 M $NaNO_3$ at 20 mV contains the plateau of the current density independent of time instead of the current maximum. This current density plateau is in the interval of times between 2.2 and 3.8 s. The reason for the absence of the current maximum lies in the fact that this overpotential belongs to the ohmic control of the electrodeposition process.

The diffusion coefficients were calculated by the linearization of the falling part of the transients applying of Cottrell equation given by Eq. (1):[34,35]

$$j = nFc\left(D/\pi\right)^{1/2} t^{-1/2} \quad (1)$$

In the Eq. (1), nF is the molar charge transferred during electrodeposition, c is the bulk concentration of the electroactive species, D is the diffusion coefficient, and t is time. For the overpotentials belonging to the diffusion parts at the polarization curves, the values of decreasing current densities after current maximum were plotted with $t^{-1/2}$, and the obtained dependencies for various concentrations of the supporting electrolytes are presented in Fig. 3. The beginning of the validity of Cottrell equation, *i.e.*, the linearization from the origin shifts towards the lower overpotentials of electrodeposition with the increasing $NaNO_3$ concentration. It is clear that the linear dependence of j on $t^{-1/2}$ from the origin denotes that the full diffusion control of the electrodeposition process was attained. The absence of the linearization from the origin, *i.e.*, the existence of the current density intercept at the ordinates can be ascribed to the contribution of the ohmic control to the overall control of the electrodeposition process. It is necessary to note that the size of intercept at the ordinates decreases with increasing the overpotential, as well as with the increasing $NaNO_3$ concentration at the one

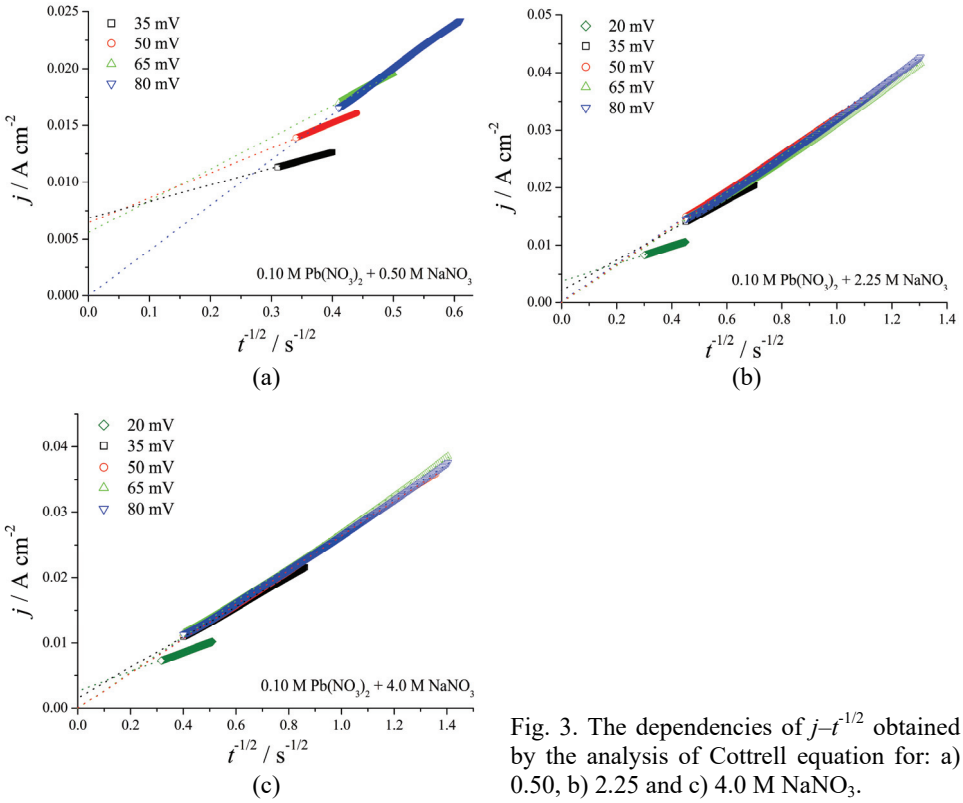

Fig. 3. The dependencies of j–$t^{-1/2}$ obtained by the analysis of Cottrell equation for: a) 0.50, b) 2.25 and c) 4.0 M $NaNO_3$.

overpotential. The decrease in the size of the intercept at the ordinates means the decrease of the contribution of the ohmic control. Hence, the beginning of the validity of Cottrell equation denotes that the effect of the ohmic control is eliminated and that the electrodeposition system became the full diffusion controlled one. The values of diffusion coefficients calculated from the slope of the linear dependencies in the range of the validity of Cottrell equation are summarized in Table I. As expected, the decrease of the diffusion coefficient values with the increasing $NaNO_3$ concentration is obtained.

TABLE I. The values of diffusion coefficients (D / 10^{-5} cm^2 s^{-1}) determined from Cottrell equation for the different concentration of $NaNO_3$; 0.10 M $Pb(NO_3)_2$

$c(NaNO_3)$ / mol m^{-3}	η / mV		
	50	65	80
0.50	–	–	1.35
2.25	0.88	0.85	0.89
4.0	0.60	0.61	0.60

The obtained diffusion coefficients were compared with those obtained by fitting the experimental chronoamperogram applying non-linear fitting procedure.[36–38] For the fitting procedure, model proposed by Scharifker *et al.*[30,39,40] based on the three-dimensional (3D) nucleation with the diffusion controlled growth was used. In this model, the current density associated with the 3D nucleation and the diffusion controlled growth is given by Eq. (2):[36]

$$j_{\text{3D-DC}}(t) = \left(\frac{nFD^{1/2}c}{\pi^{1/2}t^{1/2}}\right)\left(1-\exp\left\{-N_0\pi k' D\left[t-\frac{1-\exp(-At)}{A}\right]\right\}\right) \qquad (2)$$

In the Eq. (2), the number density of active sites is N_0, the nucleation rate constant is A, and Eq. (3) defines k':

$$k' = \frac{4}{3}\left(\frac{8\pi cM}{\rho}\right)^{1/2} \qquad (3)$$

In Eq. (3), M and ρ are the atomic weight and the density of the deposit.

The analysis of the Eq. (2) enables to determine kinetic parameters of Pb electrodeposition process and to obtain some important information related with the process of nucleation. The method of non-linear fitting using the Levenberg–Marquardt algorithm available in OriginPro was applied to determine the kinetic parameters, such as D, A and N_o. During non-linear fitting process, D, A and N_o were independent parameters. The non-linear fitting process was applied for the potentiostatic current transients obtained at the overpotentials at which the full diffusion control was attained from the electrolytes with the addition of 2.25 and 4.0 M $NaNO_3$. The results of non-linear fitting processes obtained from these

electrolytes at 50, 65 and 80 mV are shown in Fig. 4. The good superposition between the experimental potentiostatic current transients and those obtained by the non-linear fitting method using Eq. (2) was observed. This good superposition clearly indicates that the processes of nucleation/growth of Pb from the analyzed electrolytes really follow the 3D nucleation with the diffusion controlled growth. The values of parameters (D, A and N_o) obtained by non-linear fitting process are summarized in Table II.

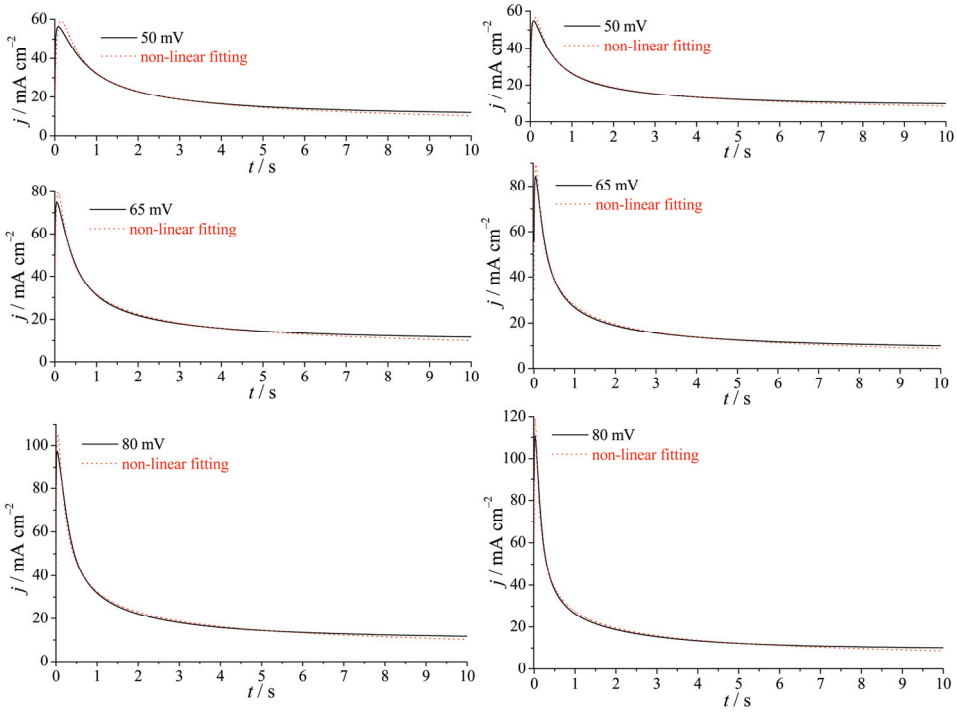

Fig. 4. The dependencies of j on t recorded at overpotentials of 50, 65 and 80 mV from 0.10 M $Pb(NO_3)_2$ in: a) 2.25 and b) 4.0 M $NaNO_3$, and the corresponding dependencies obtained through fitting process by non-linear fitting method using Eq. (2).

From Tables I and II, it can be noticed the good agreement between the diffusion coefficients determined by method of non-linear fitting and by applying of Cottrell equation for the electrolytes containing 2.25 and 4.0 M $NaNO_3$. Also, the obtained values were in the good agreement with those observed by Mostany *et al.*[30] for this type of electrolyte. The values of A and N_0 show overpotential dependence and increase with the rise in the overpotential, which is in a line with the basic law of nucleation. Namely, the nucleation rate constant, A depends on the overpotential, η as:

$$A = K_1 j_0 \exp\left(-\frac{K_2}{\eta^2}\right) \quad (4)$$

where K_1 and K_2 are overpotential-independent constants.[1] The analysis of Eq. (4) shows that increasing the overpotential causes the increase of the nucleation rate constant, which is experimentally proved (Table II). Simultaneously, the obtained values of A were considerably larger than those observed during nucleation of Cu[36] and Co[41]. It is understandable because Pb belongs to the group of *normal* metals[2,3] characterized by the large values of the exchange current density ($j_0 \rightarrow \infty$), while Cu and Co belong to the groups of the intermediate (the medium exchange current density, Cu) or inert (the low exchange current density, Co) metals.

Table II. The values of the diffusion coefficients (D), the number density of active sites (N_0), and the nucleation rate constant (A) obtained from best-fit parameters through the fitting process of the experimental $j - t$ plots using Equation (2).

$c(NaNO_3)$ / mol dm^{-3}	η / mV	D / 10^{-5} cm^2 s^{-1}	N_o / 10^5 cm^{-2}	A / 10^{-3} s^{-1}
2.25	50	0.89	10.1	0.53
	65	0.84	20.1	1.7
	80	0.89	30.1	2.0
4.0	50	0.60	20.7	0.94
	65	0.64	45.7	2.3
	80	0.63	81.7	5.0

On the other hand, overpotential dependence of N_0 can be explained as follows. The active sites have different activity or different critical overpotential in relation to the formation of nuclei.[1,42] Nuclei can be formed on those centres whose critical overpotential is lower or equal to the overpotential externally applied to the cell. Hence, the higher the applied overpotential means that the greater the number of active sites taking part in nucleation process. The number density of active sites, N_0 also depends on the exchange current density. For metals with $j_0 \rightarrow \infty$ like Pb, the radii of the screening zones are large and the N_0 is low.[1] At the low exchange current densities, the screening zones radii are low, or equal to zero, the nucleation rate is large and a thin surface film can be easily formed.[1] This is experimentally confirmed by the fact that the obtained values of N_0 for Pb were considerably smaller than those observed during Cu[36] and Co[41] nucleation.

Effect of concentration of $NaNO_3$ on morphology of electrodeposited Pb

To correlate the data obtained chronoamperometry analysis, morphologies of Pb deposits obtained by Pb electrodeposition from electrolytes containing 0.10 M $Pb(NO_3)_2$ in both 0.50 and 4.0 M $NaNO_3$ were characterized by the SEM technique.

Figure 5 shows Pb deposits obtained from 0.10 M $Pb(NO_3)_2$ in 0.50 M $NaNO_3$ at overpotentials of 20 (Fig. 5a and b), 50 (Fig. 5c and d) and 80 mV (Fig. 5e and f). From Fig. 5a and b, it can be seen thar the regular hexagonal crystals were formed during electrodeposition at an overpotential of 20 mV. Formation of the hexagonal crystals at 20 mV is expected because this overpotential belongs to the ohmic controlled electrodeposition. Namely, the hexagonal shape of crystals is the typical morphological form that is formed under the ohmic control.[9,10,29] The both, regular and irregular (precursors of dendrites) crystals, as well as the needle-like dendrites are formed at an overpotential of 50 mV belonging to the initial part of the diffusion control where the effect of ohmic control is still significant (the mixed ohmic-diffusion control; Fig. 5c and d). Finally, the two-dimensional (2D) compact dendritic forms of three-cornered shape are formed at an overpotential of 80 mV in the zone of the fast growth of current with increasing overpotential (Fig. 5e and f).

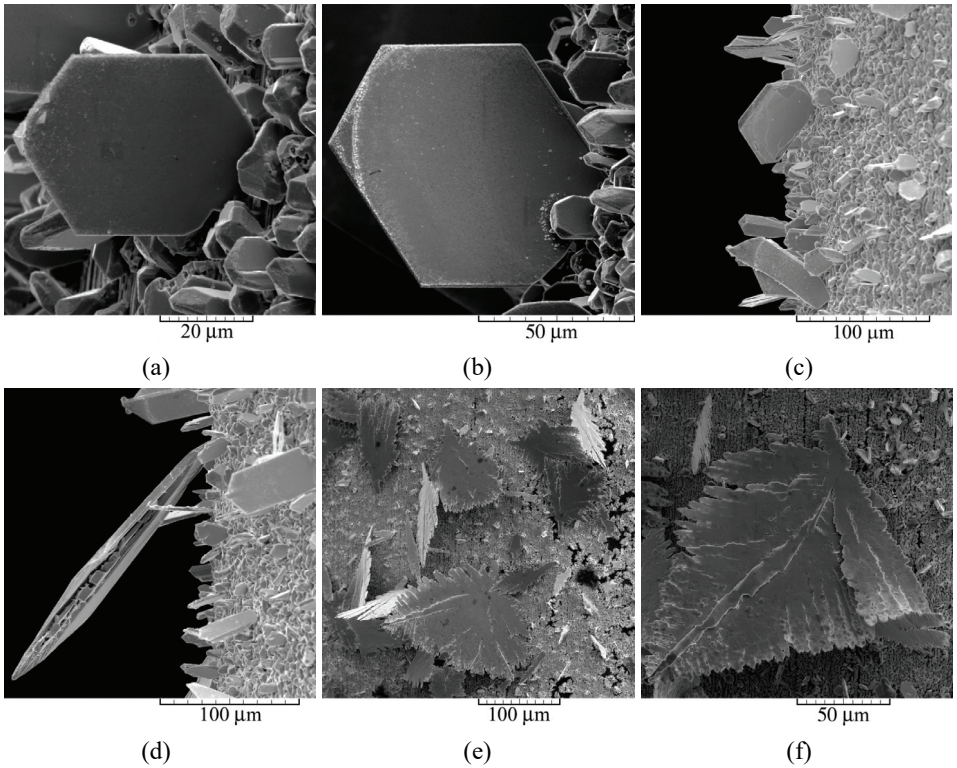

Fig. 5. Morphologies of Pb deposits electrodeposited from 0.10 M $Pb(NO_3)_2$ in 0.50 M $NaNO_3$, at overpotentials of: a) and b) 20 mV, c) and d) 50 mV, and e) and f) 80 mV.

The completely different situation was observed during electrodeposition from the solution with eight times larger concentration of the supporting elec-

trolyte. The increase of $NaNO_3$ concentration led to the decrease of the ratio of the ohmic control to the overall control of the electrodeposition process with a significant consequences on morphology of electrodeposited Pb. Morphologies of Pb deposits obtained at the same overpotentials, but from 0.10 M $Pb(NO_3)_2$ in 4.0 M $NaNO_3$ are shown in Fig. 6. Unlike of the regular hexagonal crystals formed with 0.50 M $NaNO_3$ concentration, the irregular elongated crystals (precursors of dendrites) were formed at an overpotential of 20 mV from 0.10 M $Pb(NO_3)_2$ in 4.0 M $NaNO_3$ (Fig. 6a and b). Formation of this crystal shape was understandable because an overpotential of 20 mV belongs to the part of the polarization curve when the effect of diffusion becomes significant (the mixed ohmic-diffusion control of electrodeposition). The very long needle-like dendrites were formed during electrodeposition at an overpotential of 50 mV (Fig. 6c and d). Finally, the very branchy 2D "tooth of saw" dendrites[10] were formed at an overpotential of 80 mV (Fig. 6e and f).

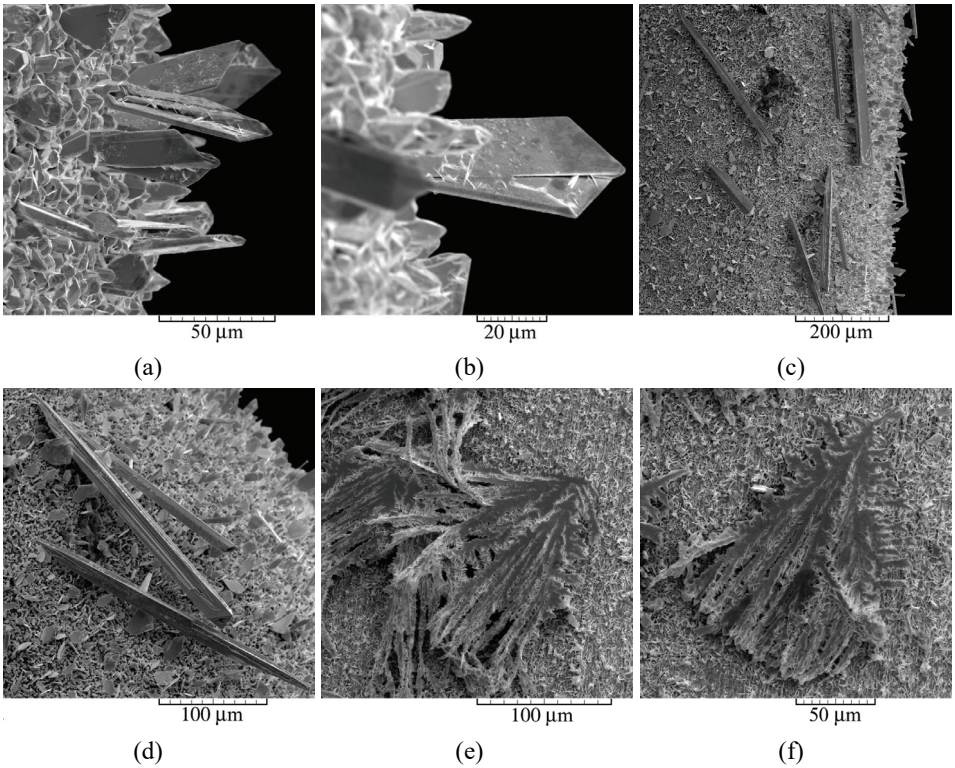

Fig. 6. Morphologies of Pb deposits electrodeposited from 0.10 M $Pb(NO_3)_2$ in 4.0 M $NaNO_3$, at overpotentials of: a) and b) 20 mV, c) and d) 50 mV, and e) and f) 80 mV.

Effect of increasing the concentration of $NaNO_3$ on polarization characteristics and morphology of electrodeposited Pb was equivalent to decreasing con-

centration of Pb^{2+} (at the constant concentration of $NaNO_3$).[10] The obtained surface morphologies are in line with data obtained by the analysis of Cottrell equation. Formation of both regular and irregular elongated crystals, as well as the needle-like dendrites from the electrolyte containing 0.10 M $Pb(NO_3)_2$ in 0.50 M $NaNO_3$ at 50 mV can be really ascribed to the electrodeposition in the mixed ohmic-diffusion control (Fig. 5c and d). The formation of only dendritic forms at 80 mV confirms that this overpotential belongs to the diffusion control of the electrodeposition (Fig. 5e and f). As far as the electrodeposition from the electrolyte with the addition of 4.0 M $NaNO_3$, the full diffusion control at 50 and 80 was confirmed by formation of both needle-like and "tooth of saw" dendrites, that is also in excellent agreement with data obtained by the analysis of Cottrell equation.

CONCLUSIONS

The kinetic parameters of Pb electrodeposition processes were determined from the analysis of chronoamperometry data and correlated with morphologies of Pb deposits obtained in the different types of electrodeposition control. The good agreement in the values of diffusion coefficients determined applying Cottrell equation and non-linear fitting method was observed. The analysis of Cottrell equation enabled to define the transition from the mixed ohmic-diffusion to the full diffusion control of electrodeposition. The values of the other parameters, such as the number density of active sites and the nucleation rate constant, obtained by non-linear fitting method assuming the three-dimensional (3D) nucleation with the diffusion controlled growth were in the accordance with the fact that Pb electrodeposition processes belong to the fast electrochemical processes characterized by the extremely high value of the exchange current density. The data obtained by the analysis of Cottrell equation were successfully confirmed by the analysis of surface morphology of lead electrodeposited at the different overpotentials. As expected, the crystals of hexagonal shape are formed during the ohmic control. Aside from this crystal type, the irregular crystals and the needle-like dendrites are formed during electrodeposition in the mixed ohmic-diffusion control. In the dependence of concentration of $NaNO_3$, the different forms of dendrites were formed during the diffusion controlled electrodeposition.

Acknowledgement. The work was supported by the Ministry of Education, Science and Technological Development of the Republic of Serbia (Project No. 172046).

ИЗВОД

ВЕЗА ИЗМЕЂУ КИНЕТИЧКИХ ПАРАМЕТАРА И МОРФОЛОГИЈЕ ЕЛЕКТРОХЕМИЈСКИ ИСТАЛОЖЕНОГ ОЛОВА

НЕБОЈША Д. НИКОЛИЋ [1], ПРЕДРАГ М. ЖИВКОВИЋ[2], САЊА И. СТЕВАНОВИЋ[1] и ГОРАН БРАНКОВИЋ[3]

[1]ИХТМ – Центар за електрохемију, Универзитет у Београду, Његошева 12, Београд, [2]Технолошко–металуршки факултет, Универзитет у Београду, Карнегијева 4, Београд и [3]Институт за мултидисциплинарна истраживања, Универзитет у Београду, Кнеза Вишеслава 1а, Београд

У овом раду су испитани процеси електрохемијског таложења олова из електролита различитих концентрација натријум-нитрата као помоћног електролита. Процеси електрохемијског таложења олова су испитани хроноамперометријом и анализом талога олова добијених у потенциостатском режиму електролизе техником скенирајуће електронске микроскопије (SEM). Постигнуто је добро слагање дифузионих коефицијената одређених из Котрелове једначине и методом нелинеарног фитовања потенциостатских струјних прелаза. По први пут, прелаз из мешовите омско-дифузионе у пуну дифузиону контролу је дефинисан из Котрелове једначине. Параметри, као што су густина активних места и константа брзине реакције, добијени методом нелинеарног фитовања су дискутовани у складу са чињеницом да олово припада групи метала окарактерисаних високим вредностима густине струје измене. Подаци добијени хроноамперометријском анализом су успешно повезани са морфологијама електрохемијски исталоженог олова добијених у различитим типовима контроле процеса електрохемијског таложења.

(Примљено 18. децембра 2015, ревидирано 12. фебруара, прихваћено 19. фебруара 2016)

REFERENCES

1. K. I. Popov, S. S. Djokić, B. N. Grgur, *Fundamental aspects of electrometallurgy*, Kluwer Academic/Plenum Publishers, New York, 2002, pp. 1–305
2. R. Winand, *Electrochim. Acta* **39** (1994) 1091
3. V. M. Kozlov, L. Peraldo Bicelli, *J. Cryst. Growth* **203** (1999) 255
4. K. I. Popov, P. M. Živković, B. Jokić, N. D. Nikolić, *J. Serb. Chem. Soc.* **81** (2016) 291
5. N. D. Nikolić, V. M. Maksimović, G. Branković, P. M. Živković, M. G. Pavlović, *J. Serb. Chem. Soc.* **78** (2013) 1387
6. E. R. Ivanović, N. D. Nikolić, V. R. Radmilović, *J. Serb. Chem. Soc.* **80** (2015) 107
7. V. M. Maksimović, N. D. Nikolić, V. B. Kusigerski, J. L. Blanuša, *J. Serb. Chem. Soc.* **80** (2015) 197
8. K. I. Popov, P. M. Živković, N. D. Nikolić, in: *Electrodeposition: Theory and Practice, Series: Modern Aspects of Electrochemistry*, S. S. Djokić, Ed., Vol. 48, Springer, 2010, pp. 163–213
9. N. D. Nikolić, G. Branković, U. Č. Lačnjevac, *J. Solid State Electrochem.* **16** (2012) 2121
10. N. D. Nikolić, K. I. Popov, P. M. Živković, G. Branković, *J. Electroanal. Chem.* **691** (2013) 66
11. C.-Z. Yao, M. Liu, P. Zhang, X. -H. He, G. -R. Li, W. -X. Zhao, P. Liu, Y. -X. Tong, *Electrochim. Acta* **54** (2008) 247
12. N. D. Nikolić, Dj. Dj. Vaštag, P. M. Živković, B. Jokić, G. Branković, *Adv. Powder Technol.* **24** (2013) 674
13. J. Mostany, J. Parra, B. Scharifker, *J. Appl. Electrochem.* **16** (1986) 333
14. A. Hazza, D. Pletcher, R. Wills, *Phys. Chem. Chem. Phys.* **6** (2004) 1773
15. D. Pletcher, R. Wills, *Phys. Chem. Chem. Phys.* **6** (2004) 1779
16. I. A. Carlos, M. A. Malaquias, M. M. Oizumi, T. T. Matsuo, *J. Power Sources* **92** (2001) 56

17. S. M. Wong, L. M. Abrantes, *Electrochim. Acta* **51** (2005) 619
18. N. D. Nikolić, Dj. Dj. Vaštag, V. M. Maksimović, G. Branković, *Trans. Nonferrous Met. Soc. China* **24** (2014) 884
19. J. Ru, Y. Hua, C. Xu, J. Li, Y. Li, D. Wang, C. Qi, Y. Jie, *Appl. Surf. Sci.* **335** (2015) 153
20. J. Ru, Y. Hua, C. Xu, J. Li, Y. Li, D. Wang, K. Gong, Z. Zhou, *Adv. Powder Technol.* **26** (2015) 91
21. N. D. Nikolić, K. I. Popov, E. R. Ivanović, G. Branković, S. I. Stevanović, P. M. Živković, *J. Electroanal. Chem.* **739** (2015) 137
22. N. D. Nikolić, E. R. Ivanović, G. Branković, U. Č. Lačnjevac, S. I. Stevanović, J. S. Stevanović, M. G. Pavlović, *Metall. Mater. Trans., B* **46** (2015) 1760
23. Y. Ni, Y. Zhang, J. Hong, *CrystEngComm* **13** (2011) 934
24. Z.-Li Xiao, C. Y. Han, W.-K. Kwok, H.-H. Wang, U. Welp, J. Wang, G. W. Crabtree, *J. Am. Chem. Soc.* **126** (2004) 2316
25. S. Cherevko, X. Xing, C.-H. Chung, *Appl. Surf. Sci.* **257** (2011) 8054
26. N. D. Nikolić, K. I. Popov, E. R. Ivanović, G. Branković, *J. Serb. Chem. Soc.* **79** (2014) 993
27. N. D. Nikolić, V. M. Maksimović, G. Branković, *RSC Adv.* **3** (2013) 7466
28. G. Wranglen, *Electrochim. Acta* **2** (1960) 130
29. N. D. Nikolić, K. I. Popov, in: *Electrodeposition and Surface Finishing, Series: Modern Aspects of Electrochemistry*, S. S. Djokić, Ed.,Vol. 57, Springer, 2014, pp. 85–132
30. J. Mostany, J. Mozota, B. Scharifker, *J. Electroanal. Chem.* **177** (1984) 25
31. J. W. Diggle, A. R. Despić, J. O` M Bockris, *J. Electrochem. Soc.* **116** (1969) 1503
32. A. R. Despić, K. I. Popov, Transport controlled deposition and dissolution of metals, in *Modern Aspects of Electrochemistry*, B. E. Conway, J. O'M. Bockris, Eds., Vol. 7, Plenum Press, New York, 1972, pp. 199–313
33. K. I. Popov, N. D. Nikolić, in: *Electrochemical Production of Metal Powders, Series: Modern Aspects of Electrochemistry*, S. S. Djokić, Ed., Vol. 54, Springer, 2012, pp. 1–62
34. J. O' M. Bockris, A. K. N. Reddy, M. Gamboa-Aldeco, *Modern Electrochemistry 2A*, 2nd ed., Kluwer/Plenum, New York, 2000, p. 1225
35. Q. B. Zang, Y. X. Hua, *Phys. Chem. Chem. Phys.* **16** (2014) 27088
36. M. Palomar-Pardavé, I. González, N. Batina, *J. Phys. Chem., B* **104** (2000) 3545
37. Q. B. Zhang, Y. X. Hua, R. Wang, *Sci. China: Chem.* **56** (2013) 1586
38. J. Ustarroz, X. Ke, A. Hubin, S. Bals, H. Terryn, *J. Phys. Chem., C* **116** (2012) 2322
39. B. Scharifker, G. Hills, *Electrochim. Acta* **28** (1983) 879
40. B. Scharifker, J. Mostany, *J. Electroanal. Chem.* **177** (1984) 13
41. L. H. Mendoza-Huizar, J. Robles, M. Palomar-Pardavé, *J. Electroanal. Chem.* **545** (2003) 39
42. R. Kaishew, B. Mutafctschiew, *Electrochim. Acta* **10** (1965) 643.